Electrochimica Acta 260 (2018) 898–904

Contents lists available at ScienceDirect

Electrochimica Acta

journal homepage: www.elsevier.com/locate/electacta

Ultrathin layered double hydroxide nanosheets with Ni(III) active species obtained by exfoliation for highly efficient ethanol electrooxidation

Liang Xu [a], Zhe Wang [b], Xu Chen [a, *], Zongkai Qu [a], Feng Li [a], Wensheng Yang [a, **]

[a] State Key Laboratory of Chemical Resource Engineering, Beijing University of Chemical Technology, Beijing, 100029, PR China
[b] Department of Chemistry, Xavier University of Louisiana, New Orleans, 70125, USA

ARTICLE INFO

Article history:
Received 4 August 2017
Received in revised form
24 November 2017
Accepted 10 December 2017
Available online 12 December 2017

Keywords:
Ultrathin layered double hydroxide nanosheets
Liquid exfoliation
Ethanol electrooxidation
Ni(III) species

ABSTRACT

The development of non-precious metal electrocatalysts for renewable energy conversion and storage is compelling but greatly challenging due to low activity of the existing catalysts. Herein, the ultrathin NiAl-layered double hydroxide nanosheets (NiAl-LDH-NSs) are prepared by simple liquid-exfoliation of bulk NiAl-LDHs and first used as ethanol electrooxidation catalysts. The ultrathin two-dimensional (2D) structure ensures that the LDH nanosheets expose a greater number of active sites. More importantly, much Ni(III) active species (NiOOH) in the ultrathin nanosheets are formed by the exfoliation process, which play an authentic catalytic role in the ethanol oxidation reaction (EOR). The presence of NiOOH remarkably improves the reactivity and electrical conductivity of LDH nanosheets. These synergistic effects lead to strikingly more than 30 times enhanced EOR activity of NiAl-LDH-NSs compared to bulk NiAl-LDHs. The obtained electrocatalytic activity is also much better than those of most Ni- and LDH-based EOR catalysts reported to date. In addition, the ultrathin NiAl-LDH-NS electrocatalyst also exhibits good long-term stability (maintain 81.8% of the original value after 10000 s). This study not only provides a highly competitive EOR catalyst, but also opens new avenues toward the design of highly efficient electrode materials that have various potential applications in supercapacitor, Ni-MH battery and other electrocatalytic systems.

1. Introduction

The increasing demand for globe energy has driven the attentions in developing clean/green alternatives to fossil fuels [1–3]. Ethanol is an attractive energy resource for fuel cells with its high energy density, low toxicity, easily storage and extensive sources [4,5]. Pt and Pt-based materials have been considered as the state-of-the-art noble-metal catalysts toward ethanol oxidation reaction (EOR) [6–9]. However, high cost, low abundance and catalytic poisoning by the carbon monoxide produced in electrooxidation have severely restricted the practical usage of Pt-based electrocatalysts in direct ethanol fuel cells (DEFCs) [10,11]. To overcome these problems, a broad range of non-precious metal catalysts have been actively pursued including metal [12], metal oxides [13], hydroxides [14] and sulfides [15]. Recently, layered double hydroxides (LDHs) have been reported as a promising candidate for various electrocatalytic systems [16–19] including EOR [18,19] owing to their novel structure and desirable properties. Nevertheless, the limited number of active sites due to the thick bulk form and the poor conductivity have hindered the further development of LDHs as EOR electrocatalysts. Several strategies such as fabricating hierarchical structured LDHs with enhanced surface area [18] and synthesizing their composites [19,20] have been developed. Although the enhanced EOR performances are obtained based on above methods, the results are still not so satisfactory for the application of DEFCs.

Actually, enhancing reactivity of active sites is another efficient approach to improve the catalyst performance, which has generally received less attention than alternating the composition or structure of the catalyst materials. For EOR based on Ni-based electrocatalysts, Ni(III) species (NiOOH) play an authentic catalytic role [12,13,20]. While generally synthesized Ni oxides and hydroxides need undergo progressive oxidation from low valence states (Ni(II))

* Corresponding author.
** Corresponding author.
E-mail address: chenxu@mail.buct.edu.cn (X. Chen).

https://doi.org/10.1016/j.electacta.2017.12.065
0013-4686/

to high valence states (Ni(III)) during electrochemical process prior to the EOR [13,14]. Previous report [21] has testified that chemically oxidized NiOOH is extremely active in electrochemical reactions. Moreover, the partial conversion of Ni(II) to Ni(III) in Ni(II)-based catalyst may also enhance the electroconductivity significantly. The electrical conductivity of chemically oxidized NiOOH is higher (10^{-5} S cm^{-1}) than that of $Ni(OH)_2$ (10^{-8} S cm^{-1}) [22]. Based on these points, directly increasing the population of high oxidation Ni species in catalysts may effectively promote the performance of EOR. Therefore, it is envisaged that substantially enhancing the OER performance may be acquired by simultaneously improving the content of Ni(III) species and exposing more active sites of LDH materials. However, the exploration of a facile and effective approach to achieve this goal remains greatly challenging.

In this work, ultrathin NiAl-LDH nanosheets (NiAl-LDH-NSs) have been prepared by one-step liquid-phase exfoliation of bulk NiAl-LDHs for electrocatalytic ethanol oxidation (Fig. 1). Owing to their ultrathin 2D structure, the NiAl-LDH-NSs expose a greater number of active sites. More interestingly, it is observed that partial Ni(II) in the layer of NiAl-LDHs were transformed to be Ni(III). The electrocatalytic performance of the resulted NiAl-LDH-NSs towards ethanol oxidation is examined systematically and compared with that of the bulk NiAl-LDHs. The dramatically enhanced activity and turnover frequency have been achieved. So far, this is the first research that exfoliated ultrathin LDH nanosheets aimed on ethanol electrooxidation, which not only expands the applications of LDH-based materials but also provides a new pathway in the exploration of high performance catalysts.

2. Experimental

2.1. Materials

Nickel(II) nitrate hexahydrate ($Ni(NO_3)_2{\cdot}6H_2O$) and aluminum(III) nitrate nonahydrate ($Al(NO_3)_3{\cdot}9H_2O$) were obtained from Sinopharm Chemical Regent Co. Ltd., China. Urea and formamide were purchased from Xilong Science Co. Ltd., China. Anhydrous ethanol and sodium hydroxides were obtained from Beijing Chemical Works (China). All other reagents were of analytical grade and used without further purification. All the aqueous solutions were prepared with deionized, doubly distilled water (DDW).

2.2. Synthesis of NiAl-LDH-NSs

The bulk NiAl-LDHs (NO_3^- intercalated) were first synthesized through a hydrothermal method [23]. 0.10 M of $Ni(NO_3)_2{\cdot}6H_2O$, 0.05 M of $Al(NO_3)_3{\cdot}9H_2O$ and 0.15 M of urea were dissolved in 80 mL of DDW that was boiled to dislodge the CO_2. The mixed solution was sonicated for 15 min to form a homogeneous solution. Then, the resulting solution was decanted to a stainless-steel Teflon-lined autoclave and heated at 190 °C for 48 h. The as-obtained green product was collected by centrifugation at 3900 rpm for 10 min, washed with boiled DDW until the solution was neutral and then anhydrous ethanol for 2 times. After drying in an oven under 60 °C overnight, the bulk NiAl-LDHs were obtained.

Subsequently, the NiAl-LDH-NSs were prepared through a mechanical liquid-exfoliation process [24]. The prepared bulk NiAl-LDHs power (0.1 g) was dispersed in 100 mL degassed formamide, and then mechanically stirred under a N_2 atmosphere for 48 h at room temperature. The resulting suspension was centrifuged at 3900 rpm for 10 min to remove a small quantity of unexfoliated particles. Then reseda transparent colloidal suspension was obtained. Finally, 10 mL obtained colloidal suspension was poured into a glass culture dish with 10 cm in diameter and dried at 60 °C overnight.

2.3. Preparation of LDH modified electrodes

Glassy carbon (GC) electrodes with a diameter of 3 mm were used as conductive substrate of the working electrode. Prior to use, the GC electrodes were polished with 1.0, 0.3, and 0.05 μm alumina slurry sequentially, followed by rinsing with DDW, sonicating and then drying by nitrogen. Then, 1.0 mg of dried bulk NiAl-LDHs or NiAl-LDH-NSs was dispersed in 1 mL of ethanol under N_2 protection and sonicated for 10 min. An aliquot (6 μL) of the bulk LDH or LDH-NS suspension was dropped on the pretreated GC electrodes. Then, the modified electrodes were coated with 2 μL of 0.2 wt% Nafion solution and dried at room temperature. Before testing, the

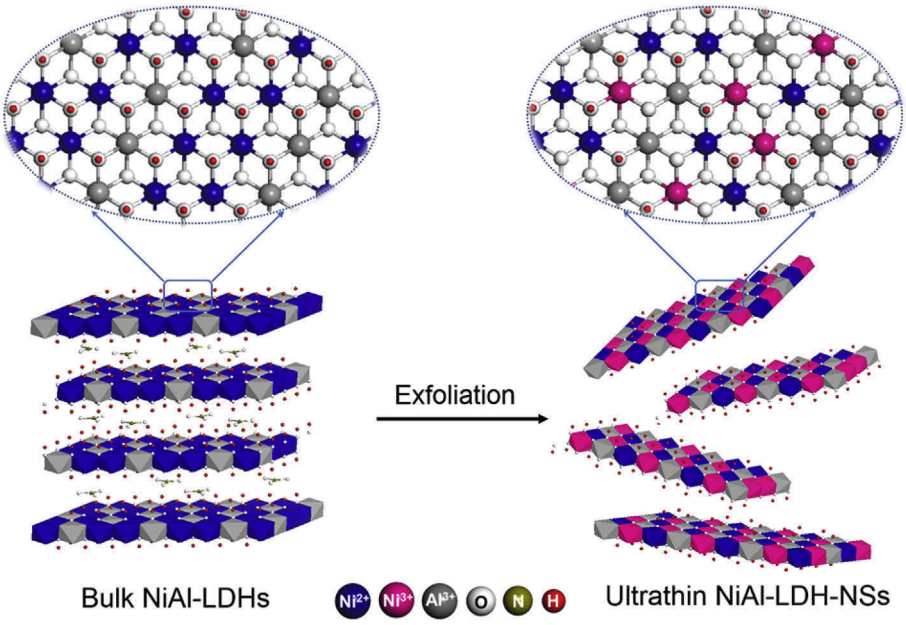

Fig. 1. Fabrication of ultrathin NiAl-LDH-NSs with Ni(III) active species.

working electrodes were electrochemically activated by cyclic scanning for 20 cycles at a potential window of 0.00–0.70 V vs. Ag/AgCl with a scan rate of 50 mV s^{-1} in 1.0 M NaOH.

2.4. Material characterization

Scanning electron microscopy (SEM) images were recorded with a Zeiss Supra 55 field emission scanning electron microscope equipped with energy-dispersive X-ray spectroscopy (EDS). Power X-ray diffraction (XRD) data were collected on a Shimadzu XRD-6000 diffractometer with Cu Kα radiation (40 kV, 30 mA, and λ = 0.154 nm). Transmission electron microscopy (TEM) images were obtained on Hitachi H-800 electron microscope and high resolution TEM (HRTEM) images were tested by a JEM-2100F transmission electron microscope with an accelerating voltage of 200 kV. The size and thickness of LDH nanosheets were determined by Atomic Force Microscope (AFM, Multimode Nanoscope IIIa, Veeco Instruments). X-ray photoelectron spectroscopy (XPS) was conducted using X-ray photoelectron spectrometer (Thermo ESCALAB 250) with Al Kα as radiation source. Liquid chromatographic analyses were performed on a Shimadzu LC-20AT with an ultraviolet (UV) detector.

2.5. Electrochemical measurements

All the electrochemical measurements were carried out in a three-electrode system using a CHI 660E electrochemical workstation (Shanghai CH Instruments, China) at room temperature. The bulk NiAl-LDH or NiAl-LDH-NS modified glassy carbon electrode was employed as the working electrode. Pt wire and Ag/AgCl (saturated KCl) were used as counter and reference electrodes, respectively. The electrolyte was 1.0 M NaOH aqueous solution. The electrochemical surface area (ECSA) values of bulk NiAl-LDH and NiAl-LDH-NS modified electrodes were measured at potential window ranges in 0.00–0.10 V, and the scan rates are 20, 40, 60, 80 and 100 mV s^{-1}, respectively. The electrochemical impedance spectroscopy (EIS) was recorded at an applied potential of 0.60 V vs. Ag/AgCl in the frequency range of 0.1–10^5 Hz with an amplitude of applied voltage of 5 mV.

3. Results and discussion

3.1. Morphological and structural characterization

The morphological and structural characterization of the as-synthesized bulk NiAl-LDHs and NiAl-LDH-NSs are shown in Fig. 2. SEM image (Fig. 2A) shows that the bulk NiAl-LDHs have a plate-like structure with a lateral size of 300–500 nm and a thickness of ~20 nm, which is further demonstrated by TEM (Fig. S1). The XRD pattern of the bulk NiAl-LDHs (Fig. 2B) exhibits a series of Bragg reflections, in good agreement with that of the NiAl-LDHs [25]. The basal spacing of 0.88 nm calculated from 2θ = 10.04° indicates the nitrate as the interlamellar anion [26]. EDS analysis (Fig. S2) confirms the composition of element and metal proportion (Ni: Al ≈ 2:1) in bulk NiAl-LDHs, which is consistent with the feed ratio in the precursor solution. These results demonstrate that the NO_3^- intercalated NiAl-LDHs have been successfully synthesized.

The ultrathin 2D NiAl-LDH-NSs are further prepared through a simple liquid-exfoliation process. After being dispersed in formamide with continuous stirring under N_2 atmosphere for 48 h, suspension of bulk NiAl-LDHs becomes clear solution (Fig. 2C). An obvious Tyndall effect is observed upon irradiation of the solution with a laser beam, indicating the exfoliation of bulk NiAl-LDHs into single layers [27,28]. A further evidence of successful exfoliation is the absence of (00*l*) peaks in the XRD pattern of NiAl-LDH-NSs (Fig. 2B). The NiAl-LDH-NSs are directly observed by TEM (Fig. 2D). NiAl-LDH-NSs possess a faint and identified contrast, further confirming its ultrathin nature. The detailed nanostructure of NiAl-LDH-NSs is also investigated by HRTEM (inset in Fig. 2D). The NiAl-LDH-NSs exhibit a hexagonal lattice with a = 0.25 nm, which is corresponding to the exposed (012) facet of the NiAl-LDH phase [29]. The existence of (012) facet indicates the exfoliated nanosheets were still crystalline, which is consistent with the XRD results (Fig. 2B). EDS result (Fig. S2) confirms that the composition of element and metal proportion in NiAl-LDH-NSs basically remained after exfoliation. Furthermore, AFM image and the height profiles (Fig. 2E and F) prove that the thickness of the obtained nanosheets is located in a range of 0.75–0.88 nm, which is consistent with the thickness of a single or double layer of LDHs [30,31]. Therefore, NiAl-LDH-NSs with well-defined 2D structure and atoms thick have been successfully prepared. The unique structure endows the material with large specific surface area and high exposure of surface atoms, which are beneficial to the further catalysis application.

The performance of EOR is significantly influenced by the surface properties of the electrocatalysts. Therefore, the surface composition and metal valence state of the samples before and after exfoliation are elucidated by XPS. Fig. 3 shows the high-resolution Ni $2p_{3/2}$ spectra of bulk NiAl-LDHs and NiAl-LDH-NSs, which are fitted and split into two different types: Ni(II) (855.9 eV) [32,33] and Ni(III) (857.2 eV) [21,34]. The bulk NiAl-LDHs exhibit a Ni $2p_{3/2}$ XPS spectrum locating at binding energy of 855.9 eV, indicating Ni atom in the host layers of bulk NiAl-LDHs mainly existed as Ni(II). After exfoliated, the peak locating of the NiAl-LDH-NSs at binding energy of 857.2 eV obviously increases, demonstrating that new Ni(III) formed in NiAl-LDH-NSs. The Ni(III) surface states in NiAl-LDH-NSs account for ~56.5%, versus ~10.7% in the bulk NiAl-LDHs. The growing amount of surface Ni(III) species in NiAl-LDH-NSs is possibly attributed to the change of the atomic environment of the Ni atoms in the layer after exfoliation into single layer [21,35]. As the Ni(III) is really active site for Ni-based EOR electrocatalysts, thus the presence of high content of Ni(III) in the ultrathin NiAl-LDH-NSs could be significantly improve their catalytic activity in the EOR.

3.2. Ethanol electrooxidation performance

Cyclic voltammetry (CV) measurement is employed to evaluate the ethanol electrooxidation activity of the obtained samples. Fig. 4A shows the CVs of NiAl-LDH-NSs and bulk NiAl-LDHs in 1.0 M NaOH solution. The NiAl-LDH modified electrode shows a pair of redox peak at 0.36 V and 0.58 V, corresponding to the typical oxidation and reduction between Ni(II) to Ni(III) [14]. For the NiAl-LDH-NS modified electrode, this pair of redox peak (peak b and b') are also observed, and much larger CV curve areas for the redox peak are obtained. This indicates that the more active sites in NiAl-LDH-NSs are exposed due to reducing the thickness of LDHs [21]. Furthermore, it is very interesting that a new pair of redox peak (peak a and a') of the NiAl-LDH-NS modified electrode appears at 0.34 V and 0.37 V, respectively (Fig. 4A), assigned to the electro-redox of NiOOH [12,36]. When 1.0 M ethanol is added into the 1.0 M NaOH solution, the NiAl-LDH-NS catalyst exhibits a large anodic peak at 0.58 V with an oxidation current density of 45.80 mA cm^{-2} (534.33 A g^{-1}) (Fig. 4B and Fig. S3), which is 39 times higher than that of the bulk NiAl-LDHs at 0.58 V (1.17 mA cm^{-2}, 13.65 A g^{-1}; Fig. 4B). Moreover, the lower onset potential of NiAl-LDH-NSs indicates a significant enhancement in the kinetics of the ethanol electro-oxidation reaction. The activity of the NiAl-LDH-NSs catalyst is further investigated in terms of the apparent turnover frequencies (TOFs) (detailed calculation shown in the supporting

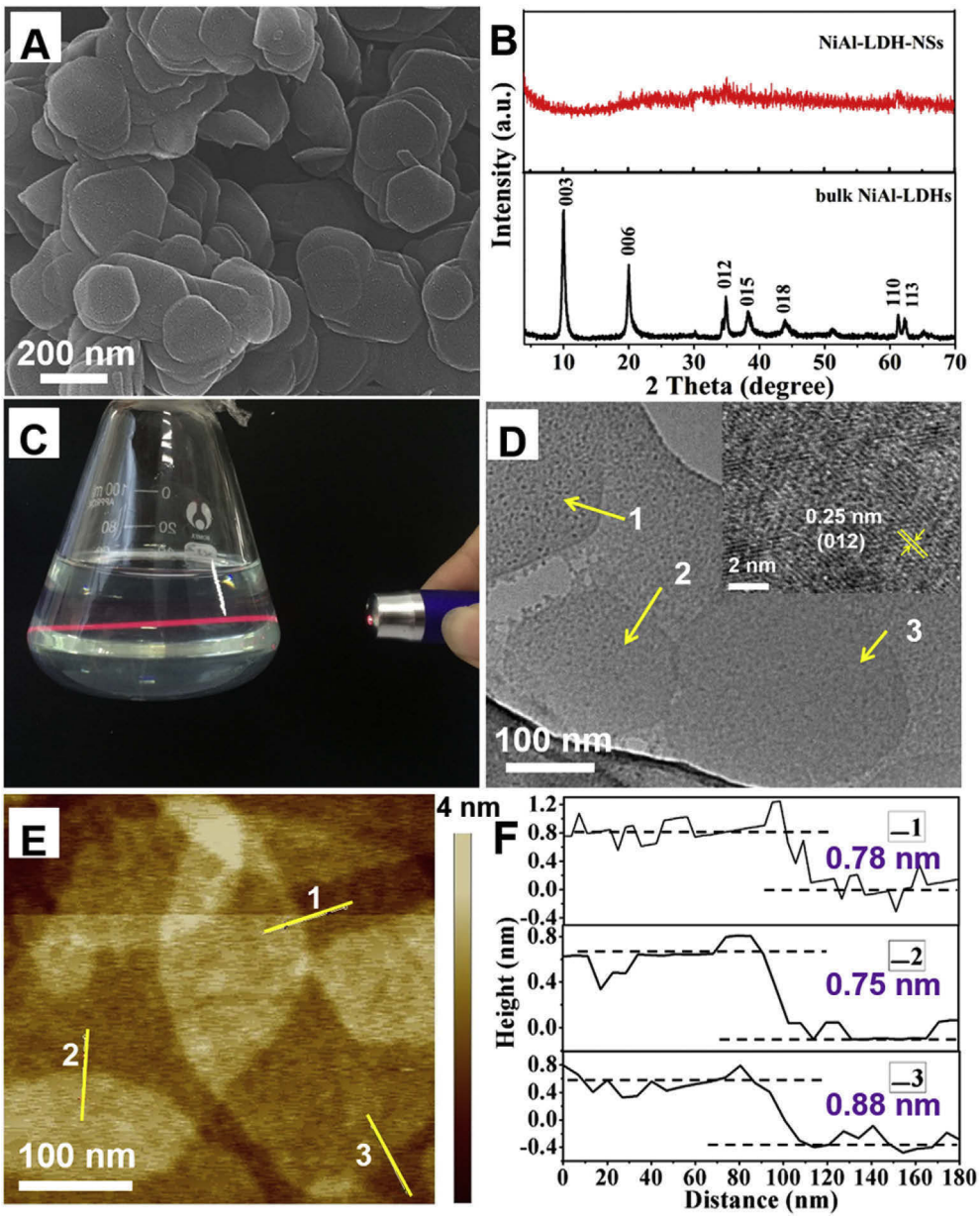

Fig. 2. (A) SEM image of bulk NiAl-LDHs. (B) XRD patterns of bulk NiAl-LDHs and NiAl-LDH-NSs. (C) Optical image of Tyndall effect of NiAl-LDH-NSs solution when irradiated with a laser beam. (D) TEM image and HRTEM image (inset) of the NiAl-LDH-NSs. (E) AFM image and (F) the corresponding height profiles for NiAl-LDH-NSs.

information). NiAl-LDH-NSs have a TOF of 0.171 s^{-1} at a potential of 0.58 mV, which is about 30 times higher than that of the bulk NiAl-LDHs (about 0.006 s^{-1}), indicating NiAl-LDH-NSs can accelerate the rate of EOR signally. Furthermore, the EOR current density of NiAl-LDH-NSs shows a linear increase with the ethanol concentration of 0.0–1.0 M (Fig. S4). These electrochemical data clearly illustrate that NiAl-LDH-NSs shows remarkably enhanced electrocatalytic activity for EOR compared to bulk NiAl-LDHs. The performance comparison with currently typical Ni-based and LDH-based catalytical systems is also given in Table 1. The NiAl-LDH-NSs also exhibit the highest current density towards the ethanol electrooxidation.

Furthermore, the products of ethanol electrooxidation reaction have been investigated by liquid chromatography (Fig. S5). The results indicate the main products of EOR with this ultrathin NiAl-LDH-NSs as electrocatalyst are acetaldehyde and acetic acid. The electrochemical measurement further proves this result. As shown in Fig. S6, the ultrathin NiAl-LDH-NSs have a good catalytic activity for acetaldehyde while have no catalytic performance for acetic acid, demonstrating the acetic acid is the final product in this reaction process. Combine the results in our work and the general reported EOR reaction mechanism by Ni-based catalysts in the literature [12,13], the EOR reaction process by ultrathin NiAl-LDH-NSs in this work is as follows:

$$Ni(OH)_2 + OH^- \rightarrow NiOOH + H_2O + e^- \quad (1)$$

$$NiOOH + CH_3CH_2OH \rightarrow CH_3CHO + Ni(OH)_2 \quad (2)$$

$$NiOOH + CH_3CHO \rightarrow CH_3COOH + Ni(OH)_2 \quad (3)$$

The long-term chronoamperometry and multiple cycle tests are

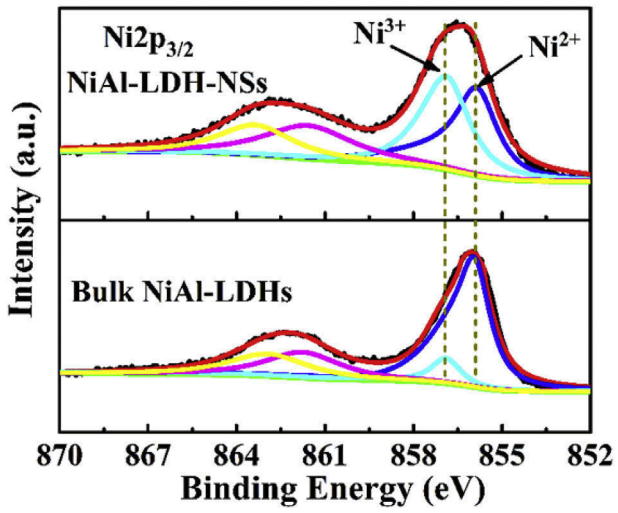

Fig. 3. Ni $2p_{3/2}$ XPS spectra of bulk NiAl-LDHs and NiAl-LDH-NSs.

carried out to assess the stability of the samples under continuous operating conditions. In Fig. 4C, the current density of the NiAl-LDH-NS modified electrode for 1.0 M ethanol is much higher than that of the bulk NiAl-LDH modified electrode, further demonstrating a significantly enhanced electrocatalytic activity. Moreover, the current density of the NiAl-LDH-NSs maintains 91.6% of its original value after 2000 s and 81.8% after 10000 s, while bulk NiAl-LDHs retains only 70.2% of its initial value after 2000 s. In addition, the NiAl-LDH-NS modified electrode also exhibits satisfactory cycling stability. As shown in Fig. 4D, 84.7% of the initial catalytic activity is still maintained after 200 potential cycles for NiAl-LDH-NSs, much better than that of bulk NiAl-LDHs (67.1%). The results demonstrate that the NiAl-LDH-NSs also showed the greatly improved stability of EOR.

3.3. Discussion of the enhanced performance

The excellent electrocatalytic performance of NiAl-LDH-NSs for EOR, especially for extraordinarily enhanced electrocatalytic activity (39 times high than that of bulk NiAl-LDHs) inspires us to further explore the possible reasons. Surface area is an important factor in catalysis; the increase of surface area is often primarily responsible for enhanced catalytic activity after nanostructuring. Hence, the enhanced surface area of exfoliated NiAl-LDH-NSs is resolved by the electrochemical surface area (ECSA). As the double-layer capacitance (C_{dl}) is linearly proportional to ECSA, here, C_{dl} of bulk NiAl-LDH and NiAl-LDH-NS modified electrodes is characterized by CV measurement method [38,39]. CV curves of these two modified electrodes in 1.0 M NaOH solution at different scan rates from 0.0 to 0.1 V (vs. Ag/AgCl) are shown in Fig. 5A and Fig. S7. From which, the plots of $\Delta j/2=(j_a-j_c)/2$ at 0.05 V (vs. Ag/AgCl) against the scan rates were obtained and shown in Fig. 5B. The C_{dl} of the NiAl-LDH-NSs is 2.8 times higher than that of the bulk NiAl-LDHs, demonstrating the larger surface area of the exfoliated nanosheets. However, the EOR performance for NiAl-LDH-NSs increases 39-fold tremendously than bulk NiAl-LDHs with 2.8-fold increase in ECSA. This testifies that the increased ECSA by the exfoliation is not the main factor for the enhanced catalytic performance.

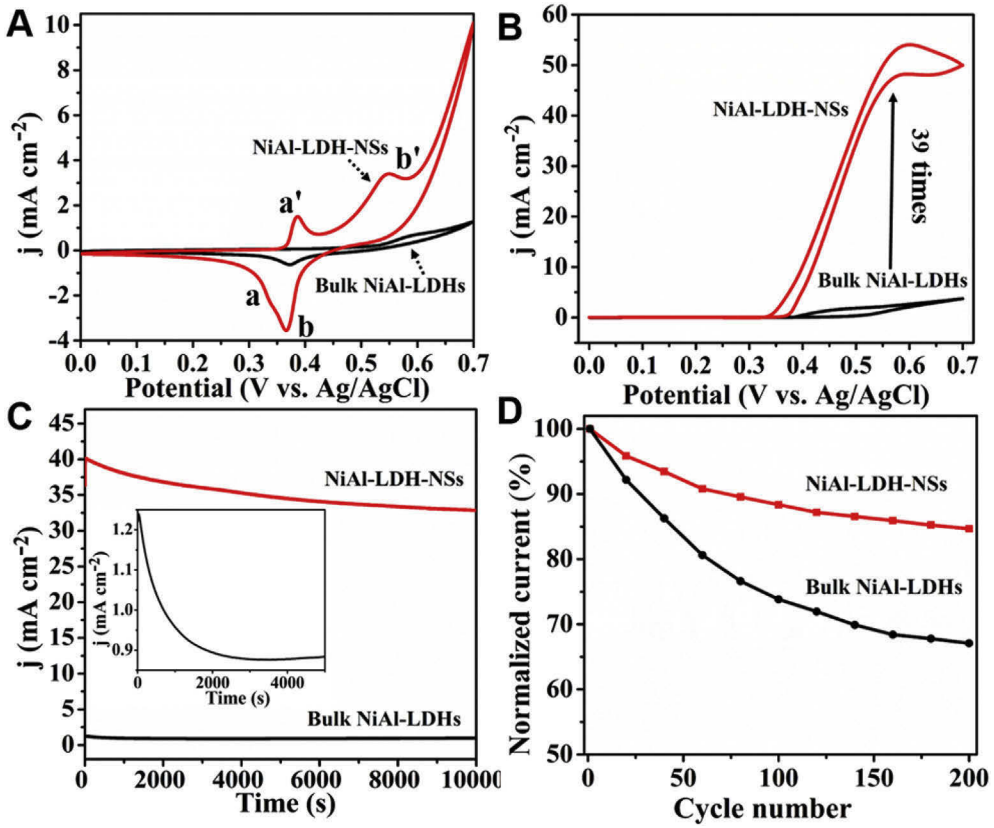

Fig. 4. CV curves of bulk NiAl-LDH and NiAl-LDH-NS modified electrodes in 1.0 M NaOH in the absence (A) and the presence of 1.0 M ethanol (B) at a scan rate of 50 mV s^{-1}. (C) Chronoamperometric curves of bulk NiAl-LDH and NiAl-LDH-NS modified electrodes in 1.0 M NaOH including 1.0 M ethanol at an applied potential of 0.58 V vs. Ag/AgCl (inset: the larger view for bulk NiAl-LDHs). (D) Cycling stability of the electrocatalytic responses for 1.0 M ethanol at bulk NiAl-LDH and NiAl-LDH-NS modified electrodes.

Table 1
Comparison of current density obtained from some Ni- and LDH-based EOR electrocatalysts in alkaline medium.

Electrocatalysts	Fuel composition	Current density (mA cm^{-2})	References
NiO	0.5 M NaOH+1.0 M ethanol	1.5	[13]
MgFe-LDH	1.0 M NaOH+1.0 M ethanol	1.14	[18]
NiFe-LDH	1.0 M NaOH+1.0 M ethanol	1.6	[19]
NiFe-LDH@MnO_2	1.0 M NaOH+1.0 M ethanol	4.5	[19]
Ni hollow spheres	1.0 M NaOH+1.0 M ethanol	17.0	[37]
NiAl-LDHs	1.0 M NaOH+1.0 M ethanol	1.17	This work
NiAl-LDH-NSs	1.0 M NaOH+1.0 M ethanol	45.8	This work

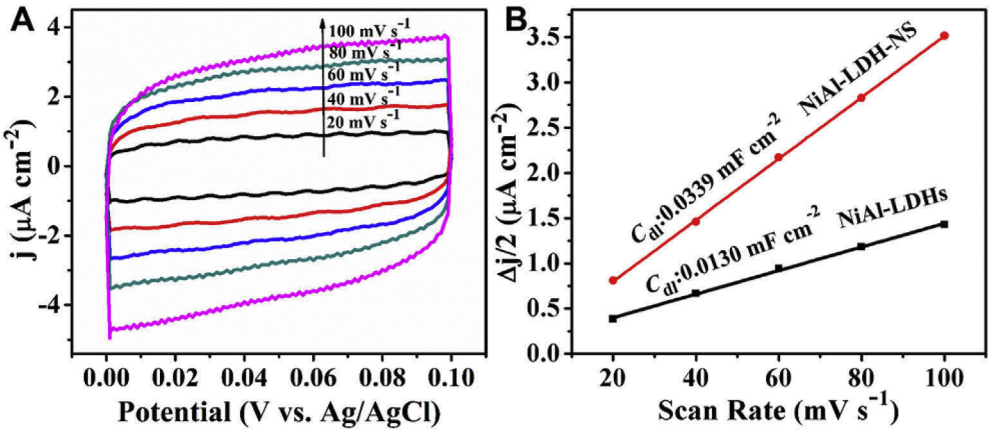

Fig. 5. (A) CV curves at different scan rates in a potential window where no Faradaic processes occur (0.0–0.1 V vs. Ag/AgCl) for NiAl-LDH-NSs on GC electrodes. (B) Charging current density differences ($\Delta j/2=(j_a-j_c)/2$) plotted against scan rates; the linear slope equivalent to the double layer capacitance C_{dl}, was used to represent the ECSA.

However, the CV curve areas and current intensity of redox peak of Ni(II) for the NiAl-LDH-NS modified electrode were much higher than that of bulk NiAl-LDH modified electrode (Fig. 5B), indicating the NiAl-LDH-NSs have a much larger number of active sites than bulk NiAl-LDHs. Therefore, exposed more active sites by exfoliation may be a main contributor for the enhanced activity of NiAl-LDH-NSs.

On the other hand, increased Ni(III) (NiOOH) content in the NiAl-LDH-NSs can be a second main contributor for higher activity. The above mentioned EOR reaction mechanism by NiAl-LDH-NSs indicates that Ni(III) (NiOOH) plays an authentic catalytic role. Directly increasing the population of high oxidation metal species Ni(III) in catalysts could effectively promote the performance of EOR. Through the exfoliation, the electrical structure of Ni ions in the layer of LDHs may be disturbed and valence state of partial nickle ions increased to higher valence. The formed Ni(III) species increases the catalyst activity of NiAl-LDH-NSs and accelerates the rate of EOR.

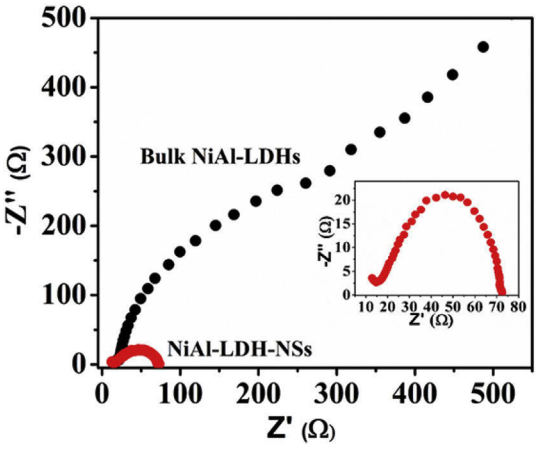

Fig. 6. Nyquist plots of bulk NiAl-LDH and NiAl-LDH-NS modified electrodes (inset: the larger view for NiAl-LDH-NSs).

In addition, the electron conductivity of the samples before and after exfoliation is investigated by electrochemical impedance spectroscopy (EIS) since it is also important factor for affecting the performance of electrocatalysis. The corresponding Nyquist plots are shown in Fig. 6. The diameter of semicircle is calculated about 60 Ω for the NiAl-LDH-NS modified electrode, which is much smaller than that of the bulk NiAl-LDHs. The EIS analysis demonstrates that the NiAl-LDH-NSs containing Ni(III) exhibit superior charge transport kinetics naturally, in accordance with previous reports [22] mentioned in the introduction. A similar phenomenon has also been reported by Pralong et al. [40,41], the chemically oxidized CoOOH had a higher conductivity compared with electrochemically oxidized CoOOH. The electrical conductivity of chemically oxidized CoOOH (10^{-2} S cm^{-1}) is actually much higher than that of electrochemically oxidized CoOOH (10^{-5} S cm^{-1}). Furthermore, the ultrathin thickness can offer an intimate contact with the electrode, and the greatly reduced interlayer distances by exfoliation can shorten the ion diffusion paths thus accelerate charge transport. Thus, improved conductivity may be another contributor for the enhanced activity of NiAl-LDH-NSs.

4. Conclusions

In summary, a highly efficient LDH-based ethanol electrooxidation catalyst is successfully synthesized through a simple liquid-exfoliation process for the first time. The as-obtained NiAl-LDH-NSs have an ultrathin 2D nanostructure (with a thickness of 0.75–0.88 nm) and a higher concentration of Ni(III) in the layer. The

excellent ethanol electrooxidation performances, including an ultrahigh current density, quick turnover frequency and long durability, are demonstrated based on the ultrathin NiAl-LDH-NSs as electrocatalysts. The tremendously enhanced EOR performance may be mainly attributed to the synergy of exposing more active sites, producing active species and improving conductivity after exfoliation. This study not only provides a competitive catalyst for ethanol electro-oxidation, but also opens a new avenue to the design of highly efficient electrode materials that have various potential applications in supercapacitor, Ni-MH battery and other electrocatalytic systems.

Acknowledgments

This work was supported by the National Natural Science Foundation of China (21521005, 21656001), Research Institute of Petroleum Processing Sinopec (216085) and Beijing Engineering Center for Hierarchical Catalysts. Z. Wang would like to acknowledge NIH funding for this work via Grant Number NIH 2G12MD007595-06, NIMHD grant number 5G12MD007595, NIGMS grant number 8UL1GM118967 and also National Science Foundation (Grant 1700429).

Appendix A. Supplementary data

Supplementary data related to this article can be found at https://doi.org/10.1016/j.electacta.2017.12.065.

References

[1] S. Chu, A. Majumdar, Opportunities and challenges for a sustainable energy future, Nature 488 (2012) 294–303.
[2] I.E. Stephens, J. Rossmeisl, I. Chorkendorff, Toward sustainable fuel cells, Science 354 (2016) 1378–1379.
[3] K. Jiang, P. Wang, S. Guo, X. Zhang, X. Shen, G. Lu, D. Su, X. Huang, Ordered PdCu-based nanoparticles as bifunctional oxygen-reduction and ethanol-oxidation electrocatalysts, Angew. Chem. Int. Ed. 55 (2016) 9030–9035.
[4] Y. Liu, S.F. Zhao, S.X. Guo, A.M. Bond, J. Zhang, Electrooxidation of ethanol and methanol using the molecular catalyst $[\{Ru_4O_4(OH)_2(H_2O)_4\}(\gamma\text{-}SiW_{10}O_{36})_2]^{10-}$, J. Am. Chem. Soc. 138 (2016) 2617–2628.
[5] L. An, T.S. Zhao, Transport phenomena in alkaline direct ethanol fuel cells for sustainable energy production, J. Power Sources 341 (2017) 199–211.
[6] R. Li, Z. Ma, F. Zhang, H. Meng, M. Wang, X.Q. Bao, B. Tang, X. Wang, Facile Cu_3P-C hybrid supported strategy to improve Pt nanoparticle electrocatalytic performance toward methanol, ethanol, glycol and formic acid electrooxidation, Electrochim. Acta 220 (2016) 193–204.
[7] B.W. Zhang, T. Sheng, Y.X. Wang, X.M. Qu, J.M. Zhang, Z.C. Zhang, H.G. Liao, F.C. Zhu, S.X. Dou, Y.X. Jiang, S.G. Sun, Platinum-cobalt bimetallic nanoparticles with Pt Skin for electro-oxidation of ethanol, ACS Catal. 7 (2016) 892–895.
[8] X. Yue, W. Yang, X. Liu, Y. Wang, C. Liu, Q. Zhang, J. Jia, A facile method to prepare $Pt/C/TiO_2$, nanotubes electrode for electro-oxidation of methanol, Electrochim. Acta 174 (2015) 667–671.
[9] W. Du, G. Yang, E. Wong, N.A. Deskins, A.I. Frenkel, D. Su, Platinum-tin oxide core-shell catalysts for efficient electro-oxidation of ethanol, J. Am. Chem. Soc. 136 (2014) 10862–10865.
[10] L. Chen, L. Lu, H. Zhu, Y. Chen, Y. Huang, Y. Li, L. Wang, Improved ethanol electrooxidation performance by shortening Pd-Ni active site distance in Pd-Ni-P nanocatalysts, Nat. Commun. 8 (2017) 14136.
[11] Y. Li, L.M. Wong, H. Xie, S. Wang, P.C. Su, Nanoporous palladium anode for direct ethanol solid oxide fuel cells with nanoscale proton-conducting ceramic electrolyte, J. Power Sources 340 (2017) 98–103.
[12] A.B. Soliman, H.S. Abdel-Samad, S.S.A. Rehim, M.A. Ahmed, H.H. Hassan, High performance nano-Ni/graphite electrode for electro-oxidation in direct alkaline ethanol fuel cells, J. Power Sources 325 (2016) 653–663.
[13] L. Calvillo, G. García, A. Paduano, O. Guillen-Villafuerte, C. Valero-Vidal, A. Vittadini, M. Bellini, A. Lavacchi, S. Agnoli, A. Martucci, J. Kunze-Liebhäuser, E. Pastor, G. Granozzi, Single-step electrophoretic deposition of non-noble metal catalyst layer with low onset voltage for ethanol electro-oxidation, ACS Appl. Mater. Interfaces 8 (2015) 716–725.
[14] J.W. Kim, S.M. Park, Electrochemical oxidation of ethanol at nickel hydroxide electrodes in alkaline media studied by electrochemical impedance spectroscopy, J. Korean Electrochem. Soc. 8 (2005) 117–124.
[15] M. Bredol, M. Kaczmarek, H.D. Wiemhöfer, Electrocatalytic activity of ZnS nanoparticles in direct ethanol fuel cells, J. Power Sources 255 (2014) 260–265.
[16] Z. Li, M. Shao, H. An, Z. Wang, S. Xu, M. Wei, D.G. Evans, X. Duan, Fast electrosynthesis of Fe-containing layered double hydroxides arrays toward highly efficient electrocatalytic oxidation reactions, Chem. Sci. 6 (2015) 6624–6631.
[17] L. Zhou, M. Shao, C. Zhang, J. Zhao, S. He, D. Rao, M. Wei, D.G. Evans, X. Duan, Hierarchical CoNi–sulfide nanosheet arrays derived from layered double hydroxides toward efficient hydrazine electrooxidation, Adv. Mater. 29 (2017) 1604080.
[18] M. Shao, F. Ning, J. Zhao, M. Wei, D.G. Evans, X. Duan, Hierarchical layered double hydroxide microspheres with largely enhanced performance for ethanol electrooxidation, Adv. Funct. Mater. 23 (2013) 3513–3518.
[19] Z. Jia, Y. Wang, T. Qi, Hierarchical Ni-Fe layered double hydroxide/MnO_2 sphere architecture as an efficient noble metal-free electrocatalyst for ethanol electro-oxidation in alkaline solution, RSC Adv. 5 (2015) 83314–83319.
[20] L.P. Jia, H.S. Wang, Preparation and application of a highly sensitive nonenzymatic ethanol sensor based on nickel nanoparticles/Nafion/graphene composite film, Sens. Actuators B 177 (2013) 1035–1042.
[21] Y. Zhao, Q. Wang, T. Bian, H. Yu, H. Fan, C. Zhou, L.Z. Wu, C.H. Tung, D. O'Hare, T. Zhang, Ni^{3+} doped monolayer layered double hydroxide nanosheets as efficient electrodes for supercapacitors, Nanoscale 7 (2015) 7168–7173.
[22] G. Barral, S. Maximovitch, F. Njanjo-Eyoke, Study of electrochemically formed $Ni(OH)_2$ layers by EIS, Electrochim. Acta 41 (1996) 1305–1311.
[23] K.W. Li, N. Kumada, Y. Yonesaki, T. Takei, N. Kinomura, H. Wang, C. Wang, The pH effects on the formation of Ni/Al nitrate form layered double hydroxides (LDHs) by chemical precipitation and hydrothermal method, Mater. Chem. Phys. 121 (2010) 223–229.
[24] F. Song, X. Hu, Exfoliation of layered double hydroxides for enhanced oxygen evolution catalysis, Nat. Commun. 5 (2014) 4477.
[25] Q. Liu, G. Fan, S. Zhang, Y. Liu, F. Li, Synthesis of uniform Ni-Al layered double hydroxide via a novel reduction–oxidation route, Mater. Lett. 82 (2012) 4–6.
[26] J. Ping, Y. Wang, Q. Lu, B. Chen, J. Chen, Y. Huang, Q. Ma, C. Tan, J. Yang, X. Cao, Z. Wang, J. Wu, Y. Ying, H. Zhang, Self-assembly of single-layer CoAl-layered double hydroxide nanosheets on 3D graphene network used as highly efficient electrocatalyst for oxygen evolution reaction, Adv. Mater. 28 (2016) 7640–7645.
[27] G. Abellán, E. Coronado, C. Martí-Gastaldo, E. Pinilla-Cienfuegos, A. Ribera, Hexagonal nanosheets from the exfoliation of Ni^{2+}-Fe^{3+} LDHs: a route towards layered multifunctional materials, J. Mater. Chem. 20 (2010) 7451–7455.
[28] J. Liang, R. Ma, N. Iyi, Y. Ebina, K. Takada, T. Sasaki, Topochemical synthesis, anion exchange, and exfoliation of Co-Ni layered double hydroxides: a route to positively charged Co-Ni hydroxide nanosheets with tunable composition, Chem. Mater. 22 (2010) 371–378.
[29] Y. Zhao, P. Chen, B. Zhang, D.S. Su, S. Zhang, L. Tian, J. Lu, Z. Li, X. Cao, B. Wang, M. Wei, D.G. Evans, X. Duan, Highly dispersed TiO_6 units in a layered double hydroxide for water splitting, Chem. Eur J. 18 (2012) 11949–11958.
[30] Z. Liu, R. Ma, M. Osada, N. Iyi, Y. Ebina, K. Takada, T. Sasaki, Synthesis, anion exchange, and delamination of Co-Al layered double hydroxide: assembly of the exfoliated nanosheet/polyanion composite films and magneto-optical studies, J. Am. Chem. Soc. 128 (2006) 4872–4880.
[31] L. Li, R. Ma, Y. Ebina, N. Iyi, T. Sasaki, Positively charged nanosheets derived via total delamination of layered double hydroxides, Chem. Mater. 17 (2005) 4386–4391.
[32] M. Hu, X. Gao, L. Lei, Y. Sun, Behavior of a layered double hydroxide under high current density charge and discharge cycles, J. Phys. Chem. C 113 (2009) 7448–7455.
[33] N.V. Kosova, E.T. Devyatkina, V.V. Kaichev, Optimization of Ni^{2+}/Ni^{3+} ratio in layered $Li(Ni,Mn,Co)O_2$ cathodes for better electrochemistry, J. Power Sources 174 (2007) 965–969.
[34] A.F. Carley, S.D. Jackson, J.N. O'shea, M.W. Roberts, The formation and characterisation of Ni^{3+}—an X-ray photoelectron spectroscopic investigation of potassium-doped Ni(110)-O, Surf. Sci. 440 (1999) L868–L874.
[35] Y. Wang, Y. Zhang, Z. Liu, C. Xie, S. Feng, D. Liu, M. Shao, S. Wang, Layered double hydroxide nanosheets with multiple vacancies obtained by dry exfoliation as highly efficient oxygen evolution electrocatalysts, Angew. Chem. Int. Ed. 56 (2017) 5867–5871.
[36] Y.F. Yuan, X.H. Xia, J.B. Wu, J.L. Yang, Y.B. Chen, S.Y. Guo, Nickel foam-supported porous $Ni(OH)_2$/NiOOH composite film as advanced pseudocapacitor material, Electrochim. Acta 56 (2011) 2627–2632.
[37] C. Xu, Y. Hu, J. Rong, S.P. Jiang, Y. Liu, Ni hollow spheres as catalysts for methanol and ethanol electrooxidation, Electrochem. Commun. 9 (2007) 2009–2012.
[38] D. Merki, H. Vrubel, L. Rovelli, S. Fierro, X. Hu, Fe, Co, and Ni ions promote the catalytic activity of amorphous molybdenum sulfide films for hydrogen evolution, Chem. Sci. 3 (2012) 2515–2525.
[39] M.A. Lukowski, A.S. Daniel, F. Meng, A. Forticaux, L. Li, S. Jin, Enhanced hydrogen evolution catalysis from chemically exfoliated metallic MoS_2 nanosheets, J. Am. Chem. Soc. 135 (2013) 10274–10277.
[40] V. Pralong, A. Delahaye-Vidal, B. Beaudoin, B. Gerand, J.M. Tarascon, Oxidation mechanism of cobalt hydroxide to cobalt oxyhydroxide, J. Mater. Chem. 9 (1999) 955–960.
[41] V. Pralong, A. Delahaye-Vidal, B. Beaudoin, J.B. Leriche, J.M. Tarascon, Electrochemical behavior of cobalt hydroxide used as additive in the nickel hydroxide electrode, J. Electrochem. Soc. 147 (2000) 1306–1313.